EVALUATION OF MEDIUM-RESOLUTION SATELLITE IMAGES FOR LAND USE MONITORING USING SPECTRAL MIXTURE ANALYSIS

Florian P. Kressler
Austrian Research Centers, Seibersdorf, Austria
florian.kressler@arcs.ac.at

C.A. Mücher,
Alterra, Wageningen, the Netherlands s
s.mucher@sc.dlo.nl

Klaus T. Steinnocher
Austrian Research Centers, Seibersdorf, Austria
Klaus.steinnocher@arcs.ac.at

H.A.M. Thunnissen
Alterra, Wageningen, the Netherlands
h.a.m.thunnissen@sc.wag-ur.nl

KEY WORDS: land cover; remote sensing; linear unmixing; multi-scale; monitoring

ABSTRACT

Keeping up-to-date land cover information and tracking changes are important tasks carried out by various national and international agencies and institutions. Satellite images are an attractive data source for these purposes as they cover large areas and are recorded on a regular basis. Continuos updating of complete data bases using high resolution data is usually prohibitively expensive, especially when done on a continental or even only national level. This paper examines the use of medium spatial resolution satellite data for basic monitoring purposes. NOAA-AVHRR, SPOT Vegetation and Resource-01 MSU-SK images, covering parts of the Netherlands, are transformed using a linear unmixing algorithm in order to derive proportions of spectrally defined land cover types. The results are compared with an existing land use data base (LGN-3) in order to evaluate how suitable the different sensors are for unmixing purposes.

1 INTRODUCTION

Satellite images are an attractive data source for land cover information for large areas. For images with a medium to low spatial resolution, a traditional pixel by pixel classification is problematic, as more than one land cover type will typically be present in one pixel (mixed pixel problem). To overcome this restriction, an unmixing approach is suggested to determine the abundance of spectrally pre-defined land cover types within each pixel. Based on pure or nearly pure pixels selected from an image, a least square unmixing algorithm is applied, resulting in so called fraction images, each showing the percentage of one land cover type across the scene. The validity of the results is determined by comparing the fraction images with the Dutch land use data base (LGN-3) (Thunnissen and Noordman, 1996). A visual analysis, as well as a classification, based on the dominatn land cover type within each pixel, is carried out.

Three different satellite sensors will be examined in this study. One sensor is the Advanced Very High Resolution Radiometer (AVHRR) aboard the National Oceanic and Atmospheric Administration (AVHRR) polar orbiting satellite. Although originally designed to monitor clouds and estimate sea surface temperatures it has already been used in a number of land cover classification studies using unmixing algorithms (e.g. Hlavka and Spanner, 1995, Quarmby et al. 1992, Holben and Shimabukuro, 1993, Shimabukuro et al. 1994, Cross et al. 1991). The second sensor is the Vegetation instrument on board the SPOT-4 satellite. Designed primarily for vegetation studies it records data in spectral bands more suitable to linear unmixing than those of NOAA-AVHRR. The third image was recorded by RESURS-01 MSU-SK multispectral scanner. The spectral resolution is similar to that of the Vegetation instrument although at a much higher spatial resolution.

Linear unmixing will be performed on each image based on spectrally pre-defined land cover types. The results will be compared with the Dutch land use data base (LGN-3) to determine how suitable the images are to derive basic land cover information by a linear unmixing procedure and their potential for regular monitoring applications.

2 DATA AND STUDY AREA

The study area covers the central and northern part of the Netherlands (Figure 1) covering approximately 33.000 km². It was selected to ensure that it is covered by all the satellite images used.
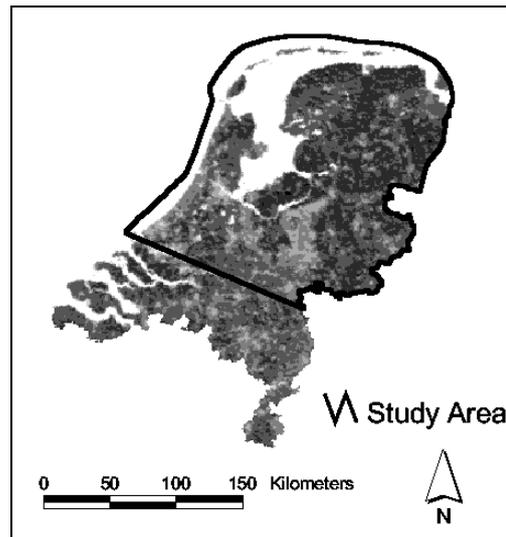
Figure 1. Vegetation band 4 image of the Netherlands with study area

Three satellite images were available for this study, one recorded by NOAA-AVHRR 14, one by SPOT-Vegetation and one by Resours-01 MSU-SK. NOAA-AVHRR records data in five spectral bands, ranging from visible red to thermal infrared, at a spatial resolution of 1100 m at nadir. SPOT Vegetation and MSU-SK have 4 bands in the visible and near infrared part of the electromagnetic spectrum with a spatial resolution of 1000 m and 170 m respectively. Table 1 shows the wavelengths of the first 4 bands for each sensors together with the names of the spectral regions (Lillesand and Kiefer, 1999).

Band #	NOAA-AVHRR 14	SPOT 4 VEGETATION	Resours-01 MSU-SK
1	0.58-0.68 (red)	0.43-0.47 (blue)	0.5-0.6 (green)
2	0.725-1.1 (near IR)	0.61-0.68 (red)	0.6-0.7 (red)
3	3.55-3.93 (mixed IR/thermal)	0.79-0.89 (near IR)	0.7-0.8 (near IR)
4	10.3-11.3 (thermal)	1.58-1.75 (mid IR)	0.8-1.1 (near IR)

Table 1. Spectral characteristics of sensors used in this study

The images were recorded on 25 July 1995 (NOAA-AVHRR), 30 July 1999 (SPOT VEGETATION) and 11 August 1997 (MSU-SK). Geocoding for NOAA-AVHRR and SPOT was carried out by the data provider based on automated routines. MSU-SK image was georefererenced using LGN3. As spectral noise was present in the entire image, a 3 x 3 median convolution filter was applied before an analysis was carried out.

As reference data the LGN-3 land use data base was used. The land use database of the Netherlands (LGN-2, an update of the first version LGN-1) was created by SC-DLO in 1995 using Landsat Thematic Mapper images of 1992 and 1994 (Thunnissen and Noordman, 1996). With respect to the production of LGN-1, newly developed classification methods were applied. Especially the new possibilities of integrating data from satellite imagery and geographical information systems have improved the quality of the database. Topographic maps, land use statistics, aerial photographs and ground reference data were used for the production of LGN-2. A multi-temporal approach provided important means for an improved classification accuracy. The resolution of the database is 25 meters. The country is covered entirely. Each pixel contains information on land use in a two level, 26 class legend. LGN-3 was created by SC-DLO in 1998 using Landsat Thematic Mapper images of 1995 and 1997 (De Wit et al., 1999). With respect to the production of LGN-3, the classification methodology used a

multi-temporal approach and was strongly based on visual interpretation. The recently available digital 1:10.000 topographic database of the Netherlands was used to add some classes which are difficult to obtain from satellite imagery. The entire country is covered with the database using a resolution 25 meters. Each pixel contains information on land use in a two level, 43 class legend. The accuracy of the database is in the order of 90% on the first level and for most classes between 70 and 90% on the second level (LGN, 2000). These classes were aggregated to five main classes representing grassland, built-up areas, forest, arable land and water.

3 METHODOLOGY

Aim of linear unmixing is to estimate how each ground pixel's area is divided between different cover types. The results are a series of images, each the size of the original image, and each giving a map of the concentration of a different cover type across the scene (Settle and Drake, 1993). Before these proportions can be calculated a set of spectra is defined called "image endmembers", representing the spectral reflectance of the different cover types. These can be defined by selecting appropriate pixel vectors, examining laboratory data or derived from a principal component analysis. When mixed using the appropriate rule, these endmembers reproduce all of the pixel spectra. The maximum number of endmembers is limited by the number of spectral bands of the satellite image.

Once the endmembers are defined the fractions of each endmember in each pixel may be calculated by applying the appropriate mixing rule. A general equation for mixing is (Adams, et al. 1989):

$$DN_c = \sum_{n=1}^{N} F_n \cdot DN_{n,c} + E_c \tag{1}$$

$$\text{where} \quad \sum_{n=1}^{N} F_n = 1 \tag{2}$$

with:
- DN_c radiance in band c,
- N number of endmembers,
- F_n fraction of endmember n,
- $DN_{n,c}$ radiance of endmember n in band c,
- E_c error for band c of the fit of N spectral endmembers.

Equation (1) converts the DN value of each pixel in each channel to the equivalent fraction (F_n) of each endmember as defined by the endmembers ($DN_{n,c}$). The error (E_c) accounts for that part of the DN-value which is not described by the mixing rule. Equation (2) introduces the constraint that the sum of all fractions must be one for each pixel.

Three ways exist to evaluate the results of the spectral mixture analysis. These are the visual analysis, the calculation of the root-mean-squared (rms) error, and the calculation of the fraction overflow (Adams et al. 1989).

With the visual analysis of the fraction images, the analyst determines whether they are consistent with other information existing about the area in question. If the patterns do not correspond with the additional information obtained by ground truthing or other sources then the model constructed may not be correct.

The second test is the calculation of the rms error. It is based on the E_c term of equation 1, squared and summed over all M image channels (see (3)) (Adams et al. 1989).

$$\varepsilon = \left[c^{-1} \sum_{c=1}^{k} E_c^2 \right]^{1/2} \tag{3}$$

with:
- ε root-mean-squared (rms) error
- k number of bands

The rms error is calculated for every pixel individually and can also be visualised as an image. It may also be calculated for the whole image, showing the overall rms error. A small rms error is an indication of a mathematically good model. A high rms error indicates that the model has not been constructed correctly.

The third test is the computation of the fraction overflow. The fractions of the land cover components should lie between zero and one, but if the model in not constructed correctly fractions may fall outside this range. As the endmembers are supposed to represent 100 % of the land cover in question, any pixel having a higher portion of the land cover as compared to the endmember pixel, will have a fraction higher than one. To satisfy the constraint that all the fractions of a pixel must sum to one, another fraction of this pixel will be below zero.If the model is not satisfactory according to the tests described above, the endmembers must either be changed, deleted, or additional endmembers defined. The following rules aid in the selection of new endmembers. An overflow in a fraction image is an indication for a pixel, which represents the land cover better then the pixel used for the definition of this endmember up to now. An overflow and a high rms error in a pixel may be due to an unmodelled endmember which is represented by that pixel (Adams et al. 1989).

4 RESULTS

For each satellite image a set of spectra was defined representing different land cover types. For the MSU-SK and VEGETATION images pixels were selected representing built-up areas, grassland and arable land. In addition an spectra representing 'shade' was defined by a zero vector. For the NOAA-AVHRR image four land cover types (in addition to the previous three forest has been added) were defined. This was possible due to the spectral information contained in the thermal band.As water could not be included as an endmember, it was masked. For the AVHRR image the water mask supplied by data provider was used. For the Vegetation and the MSU-SK a threshold was applied to the fourth band, which lies in the infrared part of the electromagnetic spectrum, to create a water mask. The water masks were applied before linear unmixing was carried out. The results are four fraction images for each image, each set representing similar land cover types. In order to evaluate the results, a visual comparison between the fraction images derived from the satellite images and an fraction image, derived from the recoded LGN 2 data set, will be performed. This is followed by a classification based on the maximum proportion of each endmember in each pixel.

Figures 2 – 5 show the fractions images for arable land derived from LGN-3 data base, SPOT Vegetation, NOAA-AVHRR and MUS-SK. Dark colors indicate low fractions and light colors indicate high fractions. It can be seen that all fraction images show very similar patterns for arable land.
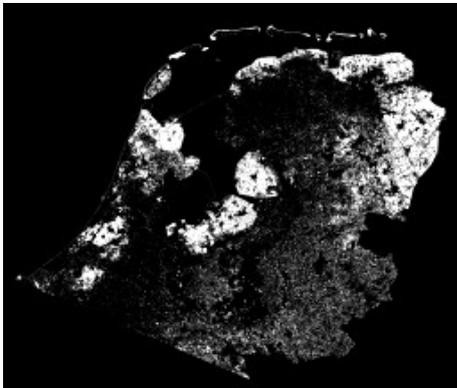
Figure 2. Fraction for arable land (LGN-3)
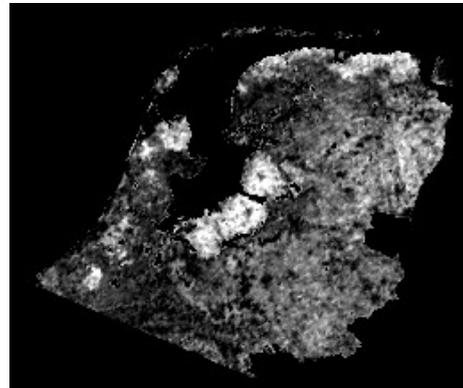
Figure 3. Fraction for arable land (Vegetation)
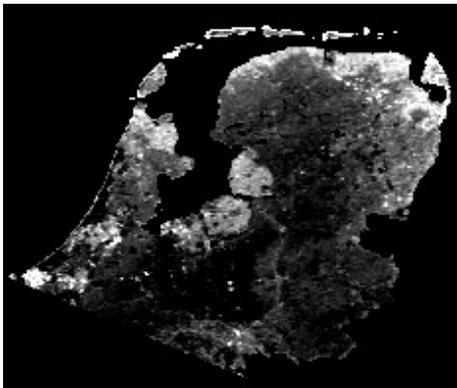
Figure 4. Fraction for arable land (AVHRR)
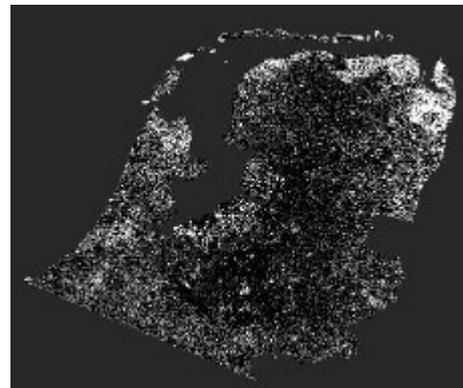
Figure 5. Fraction image for arable land (MSU-SK)

Figures 6 – 9 show the fraction images for grassland. Again the general distribution within each image is ver similar.
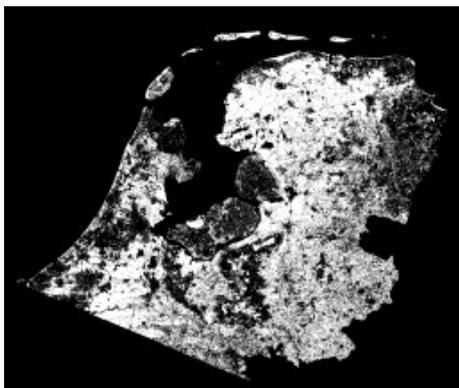
Figure 6. Fraction for grassland (LGN-3)
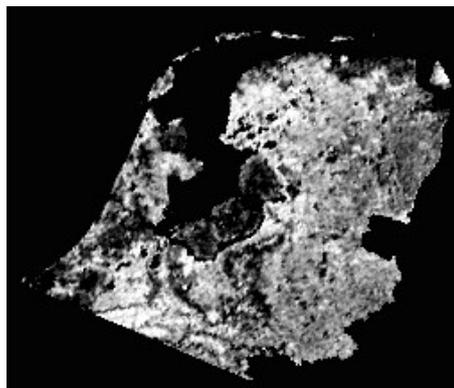
Figure 7. Fraction for grassland (Vegetation)
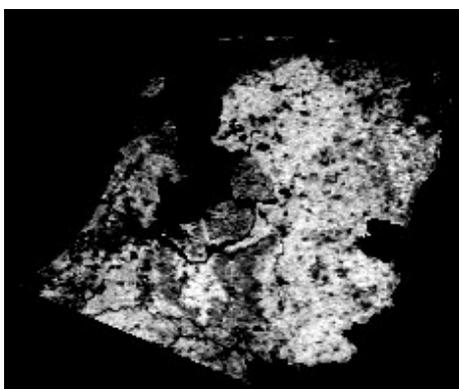
Figure 8. Fraction for grassland (AVHRRA)
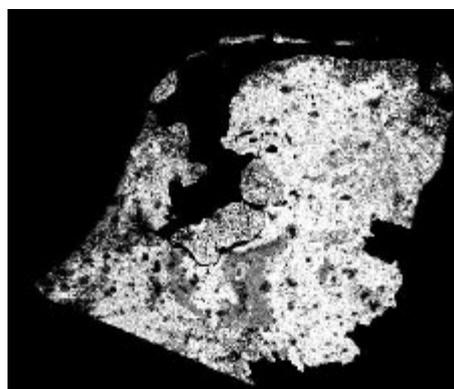
Figure 9. Fraction image for grassland (MSU-SK)

The fraction images for urban areas (figures 10-13) show larger differences. In the fraction image derived from NOAA-AVHRR the patterns of urban agglomerations are readily apparent, as they are to a lesser extent form the Vegetation fraction image. The fraction image derived from MSU-SK is comparably poor.

Figure 10. Fraction for urban areas (LGN-3)
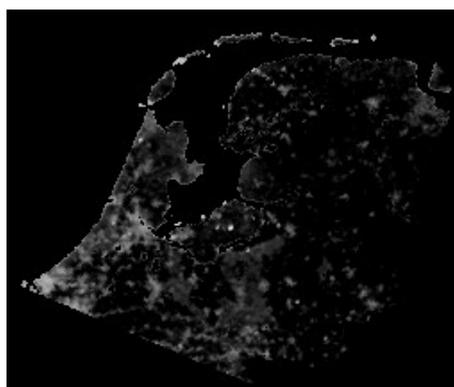
Figure 11. Fraction for urban areas (Vegetation)
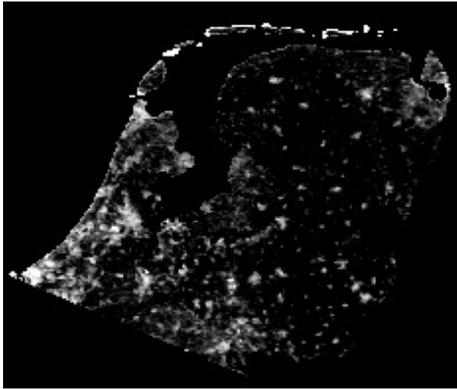
Figure 12. Fraction for urban areas (AVHRR)
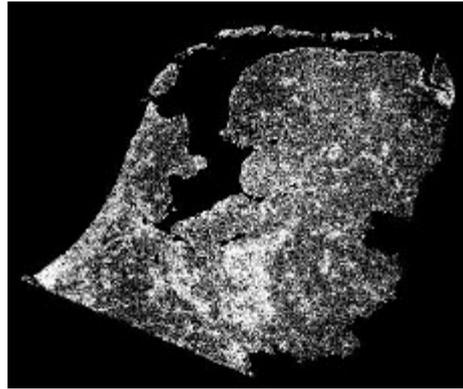
Figure 13. Fraction image for urban areas (MSU-SK)

A fraction image for forest could only be defined for the NOAA-AVHRR image. For the other images the shade-fraction image can give some indication about the distribution of forest. The fractions images from Vegetation and NOAA-AVHRR show forest along the shoreline and along canals, which is due to pixels, which contain some amounts of water but have not been masked out. This effect is less pronounced in the MSU-SK fraction image.
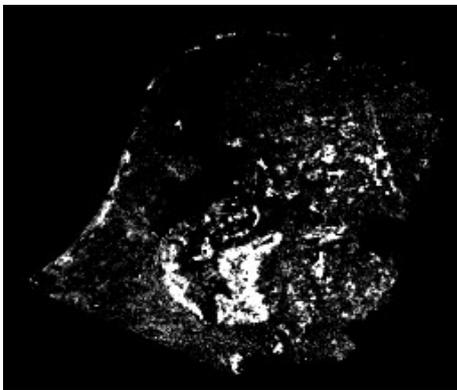
Figure 14. Fraction for forest (LGN-3)
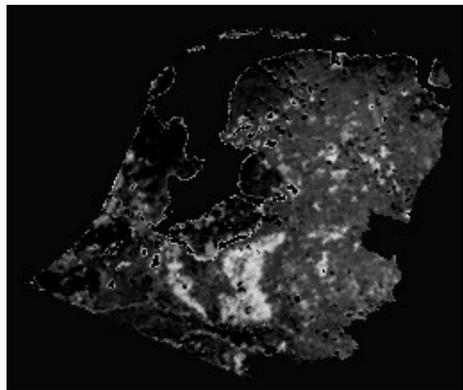
Figure 15. Fraction for shadow (Vegetation)
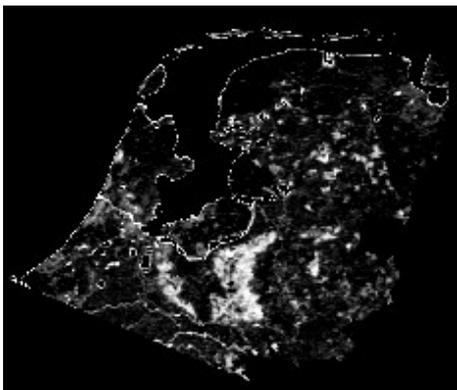
Figure 16. Fraction for forest (AVHRR)
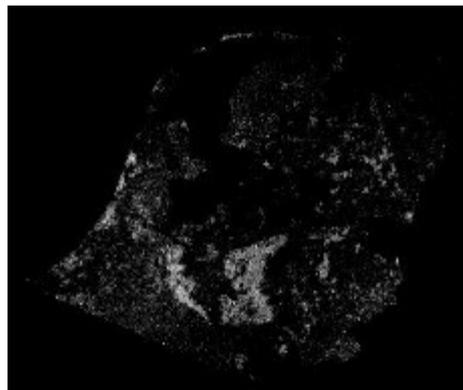
Figure 17. Fraction image for shadow (MSU-SK)

In order to compare the results of the umixing procedure for each sensor, a classification based on the maximum outtput of each fraction image was performed (figures 19 – 21). As the fraction images for forest could not be defined for Vegetation and MSU-SK, the forest pixels were determined by thresholding the shadow-fraction image.
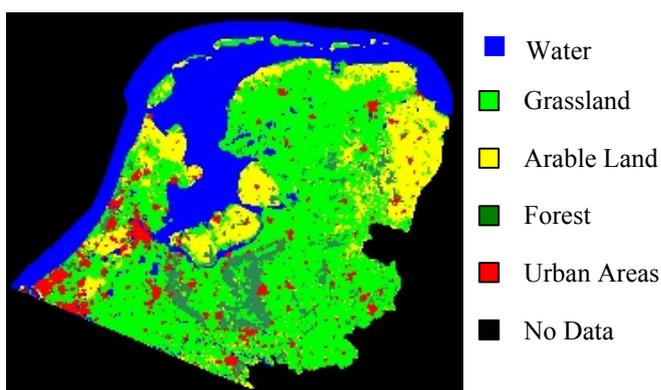
Figure 18. Classified fraction images (LGN-3)
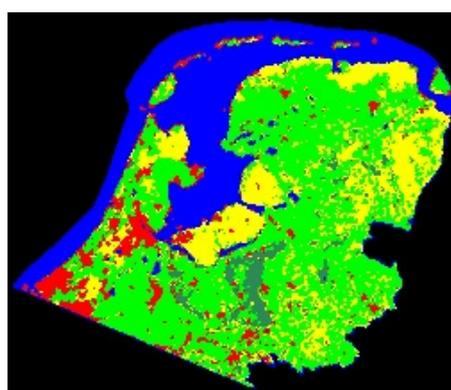
Figure 19. Classified fraction images (Vegetation)

Water
Grassland
Arable Land
Forest
Urban Areas
No Data
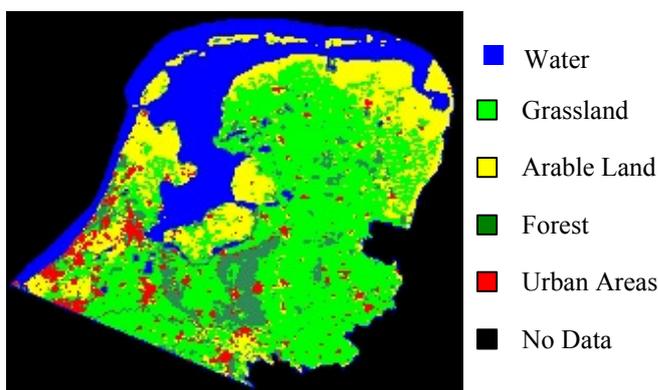
Figure 20. Classified fraction images (AVHRR)
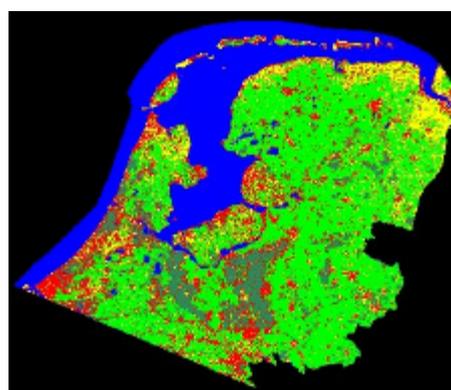
Figure 21. Classified fraction images (MSU-SK)

Water
Grassland
Arable Land
Forest
Urban Areas
No Data

The general class distribution for AVHRR and Vegetation is very similar to LGN-3. MSU-SK seems to perform rather poor for urban areas and arable land – overestimated the former and underestimating the latter. In order to evaluate the overall classification results the reference data was recoded to the resolution of each of the satellite sensors and the total number of pixels assigned to each class was calculated (Table 2).

Class	LGN-3	AVHRR		LGN-3	MSU-SK		LGN-3	Vegetation	
grassland	12.919	11.868	92%	483.498	479.876	99%	15.482	14.630	94%
urban areas	1.610	1.367	85%	75.827	168.333	222%	1.974	2.483	126%
forest	1.737	2.583	149%	87.440	103.377	118%	2.145	1.327	62%
arable land	4.034	5.350	133%	188.433	111.566	59%	4.924	6.333	129%
water	7.058	6.212	88%	292.586	264.725	90%	8.482	8.263	97%

Table 2. Agreement between LGN2 database and classification results given in number of pixels classified

The highest agreement of all sensors exists for grassland ranging from 92 % (AVHRR) to 99 % (MSU-SK). Urban areas are underestimated for AVHRR (85 %) while overestimated for MSU-SK (222 %)and Vegetation (126 %). Forests are overestimated by AVHRR (149 %) and MSU-SK (118 %) and underestimated by Vegetation (62). Arable land is overestimated by AVHRR (133 %) and Vegetation (129 %) while underestimated by MSU-SK (59 %). Water is underestimated for all sensors, ranging form 99 % (AVHRR) to 97 % for Vegetation.

The overall classification accuracy (Table 3) ranges from 63,9 % for AVHRR to 67,6 % (MSU-Sk) and 77,3 % (Vegetation).

Sensor	Overall classification accuracy (%)
NOAA-AVHRR	63,9
MSU-SK	67,6
SPOT Vegetation	77,2

Table 3. Overall classification accuracy

These results can be partially explained by the superior geometric accuracy of SPOT Vegetation over NOAA-AVHRR. The accuracy for MSU-SK with a spatial resolution of 170 m is fairly low. Here the higher spatial resolution is less relevant as the generalizing effect of a lower resolution is lost (Fisher, 1997). Also the data quality, which is rather poor due to noise may have led to a lower accuracy than would otherwise be expected.

5 CONCLUSIONS AND OUTLOOK

This paper examined the use of a linear umixing algorithm for deriving basic land cover information from multispectral sensors with a medium to low spatial resolution. Based on the overall classification accuracy derived from a classification based on fraction images, the best results could be obtained using SPOT Vegetation data. Classification accuracies derived from MSU-SK and NOAA-AVHRR data are considerably lower. For regular monitoring purposes, SPOT Vegetation offers the advantage a constant spatial resolution over the entire image compared to NOAA-AVHRR. It is expected that classification results can be improved by examining more than one image within a growing period.

6 REFERENCES

Adams, J.B., Milton, and Gillespie, A.R., 1989. Simple models for complex natural surfaces: a strategy for the hyperspectral era of remote sensing. IGARRS '89 12th Canadian Symposium on Remote Sensing, Vancouver, B.C., pp. 16-21.

Cross, A.M., Settle, J.J., Drake, N.A., and Paivinen, R.T.M., 1991. Subpixel measurement of tropical forest cover using AVHRR data. International Journal Remote Sensing, 12(5), pp. 1119-1129.

Fisher, P. 1997. The pixel: a snare and a delusion, International Journal of Remote Sensing, 18(3), pp. 679-685.

Hlavka, C.A. and Spanner, C.A., 1995. Unmixing AVHR imagery to assess clearcuts and forest regrowth in Oregon, IEEE Transactions on Geoscience and Remote Sensing, 33(3), pp. 788-795.

Holben, B.N. and Shimabukuro Y.E., 1993. Linear mixing model applied to coarse spatial resolution data from multispectral satellite sensors, International Journal Remote Sensing, 14(11), pp,. 2231-2240.

LGN, 2000. The LGN Webpage, Centre for Geoinformation, Wageningen, the Netherlands. http://cgi.girs.wageningen-ur.nl/cgi/projects/lgn/index_uk.htm

Lillesand, T.M. and Kiefer, R.W., 1999. Remote Sensing and Image Interpretation. John Wiley & Sons, New York.

Quarmby, N.A., Townshend, J.R.G. , Settle, J.J. , White, K.H. , Milnes, M. , Hindle, T.L., and Silleos, N. , 1992. Linear mixture modelling applied to AVHRR data for crop area estimation. International Journal Remote Sensing, 13(3), pp. 415-425.

Shimabukuro Y.E., Holben B.N., Tucker, C.J., 1994. Fraction images derived from NOAA AVHRR data for studying the deforestation of the Brazilian Amazon. International Journal Remote Sensing, 15(3), pp. 517-520.

Thunnissen, H.A.M. and Noordman, E., 1996. Classification methodology and operational implementation of the land cover database of the Netherlands". DLO Winand, Staring Centre, Wageningen, the Netherlands .

Thunnissen, H.A.M. and E. Noordman, 1997. Classification methodology and operational implementation of the land cover database of the Netherlands. Report 124, DLO-Winand Staring Centre, Wageningen, the Netherlands.

Wit, A.J.W. de, Th.G.C. van der Heijden and H.A.M. Thunnissen, 1999. Vervaardiging en nauwkeurigheid van het LGN3-grondgebruiksbestand. Rapport 663, DLO-Winand Staring Centre, Wageningen, the Netherlands.